Zeeman Effects in the Chlorine Nuclear Quadrupole Resonance in Sodium Chlorate*

YU TING, EDWARD R. MANRING, AND DUDLEY WILLIAMS
The Ohio State University, Columbus, Ohio

(Received May 21, 1954)

The Zeeman splitting of Cl^{35} nuclear quadrupole resonance lines in a single crystal of sodium chlorate has been studied in a magnetic field sufficiently large to permit detailed investigation of individual Zeeman components for various orientations of the crystal in the applied magnetic field. The observed patterns are in agreement with theoretical predictions based on a Hamiltonian involving an interaction of the nuclear electric quadrupole moment with a crystalline field having axial symmetry and the interaction of the nuclear magnetic moment with the applied magnetic field. The quadrupole interaction term e^2Qq was found to be 58.806 ± 0.002 Mc/sec and the effective nuclear magnetic moment was found to be 0.8215 ± 0.0001 nuclear magnetons. An upper limit for the electric asymmetry parameter η was found to be 0.0012. The intensity variations of individual Zeeman components for different orientations of the crystal relative to the magnetic field were studied. The line width of individual Zeeman components was of the order of 900 cps.

I. INTRODUCTION

A NEW field of radio-frequency spectroscopy was opened by Dehmelt and Kruger[1] when they observed direct transitions between nuclear quadrupole levels in solids. Since this early work, investigations of the subject have been made in many laboratories.[2,3] Extensive studies of chlorine nuclear quadrupole resonances in many crystals have been carried on and have yielded exact determinations of the ratio Q^{35}/Q^{37} for the nuclear quadrupole moments as well as precise measurements of the quadrupole coupling constants e^2Qq for various crystals.

The quadrupole resonance line in sodium chlorate $NaClO_3$ has been observed by Wang *et al.*[4]; this resonance line is intense and relatively narrow at room temperature. The effects of an external magnetic field on this line have been studied by Livingston[5] and by Manring,[6] who observed the Zeeman effect in a field of approximately 50 gauss.

The purpose of the present study was the investigation of the Zeeman splitting of the Cl^{35} line in $NaClO_3$ in very strong magnetic fields. By applying strong magnetic fields it is possible to separate the Zeeman components sufficiently to make accurate observations of the behavior of individual components as the magnetic field is varied and as the orientation of the crystal with respect to the magnetic field is changed. Thus, it is possible to test more precisely existing theories of the Zeeman effect.

II. THEORY

The problem of a nuclear quadrupole system coupled to a crystalline electric field and further subjected to an externally applied magnetic field has been discussed by several authors. Pound[3] and Volkoff[7] treated the case in which the quadrupole interaction is smaller than the magnetic interaction. The reverse case, in which the magnetic interaction is smaller has been treated by Kopfermann[8] and Bersohn.[9] A more general treatment has been given by Dean,[10] whose notation will be employed here.

The total Hamiltonian of a nucleus interacting with a uniform magnetic field **H** and with the gradient tensor of an electrostatic field is

$$\begin{aligned}\mathcal{H}=&\frac{e^2qQ}{4I(2I-1)}[3\mathcal{I}_z^2-\mathcal{I}^2+\tfrac{1}{2}\eta(\mathcal{I}_+^2+\mathcal{I}_-^2)]\\&-g\beta_n(H_x\mathcal{I}_x+H_y\mathcal{I}_y+H_z\mathcal{I}_z)\\=&-\delta[\mathcal{I}_z^2+\tfrac{1}{6}\eta(\mathcal{I}_+^2+\mathcal{I}_-^2)+2\xi\mathcal{I}_H]+\tfrac{1}{3}\delta\mathcal{I}^2,\end{aligned}\tag{1}$$

where $\delta=-3e^2qQ/[4I(2I-1)]$ is a measure of the electric quadrupole interaction; $\xi=g\beta_nH/2\delta$ is the ratio of magnetic interaction to electric quadrupole interaction; $\eta=(V_{xx}-V_{yy})/V_{zz}$ is the asymmetry factor of the electrostatic field; x, y, z are the principal axes of the gradient tensor of the electrostatic field; and $\mathcal{I}_\pm=\mathcal{I}_x\pm i\mathcal{I}_y$. It is assumed that η and ξ are much smaller than 1.

In the representation of eigenstates $|m\rangle$, the eigenstates of $\mathcal{I}_z$, the matrix elements of the Hamiltonian

* Supported by a contract between the O.S.U. Research Foundation and the Office of Scientific Research of the Air Research and Development Command, United States Air Force, Baltimore, Maryland.

[1] H. G. Dehmelt and H. Kruger, Naturwiss. **37**, 111 (1950); **37**, 398 (1950); Z. Physik **129**, 401 (1951).

[2] R. Livingston, Phys. Rev. **82**, 289 (1951); J. Chem. Phys. **19**, 803 (1951).

[3] R. V. Pound, Phys. Rev. **79**, 685 (1950); **82**, 343 (1951).

[4] Wang, Townes, Schawlow, and Holden, Phys. Rev. **86**, 809 (1952).

[5] R. Livingston, Science **118**, 61 (1953).

[6] E. R. Manring, Doctoral dissertation, Ohio State University, June, 1953; paper presented at Molecular Structure Symposium, Columbus, Ohio, June, 1953 (unpublished).

[7] G. N. Volkoff, Can. J. Phys. **31**, 820 (1953).

[8] H. Kopfermann, Physica **17**, 386 (1951).

[9] R. Bersohn, J. Chem. Phys. **20**, 1505 (1952).

[10] C. Dean, Doctoral dissertation, Harvard University, 1952 (unpublished).

(1) are, for $I=\frac{3}{2}$,

$$\|\langle m|\mathcal{H}|n\rangle\|=-\delta\cdot\begin{array}{|cccc|l}\multicolumn{4}{c}{(3/2)\quad(1/2)\quad(-1/2)\quad(-3/2)}&\\ 1+3\xi\cos\theta & \sqrt{3}\sin\theta\cdot e^{-i\phi} & \eta/\sqrt{3} & 0 & (3/2)\\ \sqrt{3}\xi\sin\theta\cdot e^{i\phi} & -1+\xi\cos\theta & 2\xi\sin\theta\cdot e^{-i\phi} & \eta/\sqrt{3} & (1/2)\\ \eta/\sqrt{3} & 2\xi\sin\theta\cdot e^{i\phi} & -1-\xi\cos\theta & \sqrt{3}\xi\sin\theta\cdot e^{-i\phi} & (-1/2)\\ 0 & \eta/\sqrt{3} & \sqrt{3}\xi\sin\theta\cdot e^{i\phi} & 1-3\xi\cos\theta & (-3/2),\end{array} \tag{2}$$

where θ, ϕ are the polar coordinates of $\mathbf{H}$ with respect to x, y, z, and where the constant term $\frac{1}{3}\delta\mathcal{I}^2$ is discarded. The eigenvalues E of this matrix, expressed in units of $(-\delta)$, will be given for the following cases:

(i) In the absence of an external magnetic field,

$$E=\pm(1+\tfrac{1}{3}\eta^2)^{\frac{1}{2}} \qquad (|m|=\tfrac{1}{2},\tfrac{3}{2}). \tag{3}$$

The transition frequency between these two pure quadrupole levels is then

$$f_0=(2|\delta|/h)(1+\tfrac{1}{3}\eta^2)^{\frac{1}{2}}, \tag{4}$$

where η may or may not be zero. If the electrostatic field to which the nuclear quadrupole is coupled is a crystalline field, f_0 is temperature-dependent.

(ii) For a nonzero magnetic field parallel to the z axis,

$$E=\begin{cases}[(1\pm2\xi)^2+\frac{1}{3}\eta^2]^{\frac{1}{2}}\pm\xi,\\ -[(1\mp2\xi)^2+\frac{1}{3}\eta^2]^{\frac{1}{2}}\mp\xi.\end{cases} \tag{5}$$

When $\eta=0$, this reduces to

$$E=\begin{cases}1\pm3\xi & (m=\pm\frac{3}{2}),\\ -1\pm\xi & (m=\pm\frac{1}{2}).\end{cases} \tag{5a}$$

These four levels, hereafter labeled as D, C, B, A, correspond to the four points at $\theta_A=0$ in Fig. 1. The zero magnetic field line is split into two components with frequencies

$$f_{BD,\,AC}=(2\delta/h)(1\pm\xi), \quad (\eta=0,\,\delta>0) \tag{6}$$

$$=f_0(1\pm f_M/f_0)=f_0\pm f_M, \tag{7a}$$

where $f_M=2\delta\xi/h=g\beta_n H/h$ is the magnetic resonance frequency for the nucleus in question. When $\eta\neq0$, the two Zeeman components are slightly shifted to higher frequencies:

$$f_{BD,\,AC}=f_0[1\pm(f_M/f_0)+\tfrac{2}{3}\eta^2(f_M/f_0)^2 +\text{higher powers of }\eta\text{ and }(f_M/f_0)]. \tag{7b}$$

The expansion is possible because ξ, η are assumed much smaller than 1.

(iii) For a nonzero magnetic field oriented at angle θ (except 90°) to the symmetry axis of an electric field ($\eta=0$),

$$E_{[\frac{1}{2}]B,\,[\frac{1}{2}]A}=-\Big[1\mp(1+3\sin^2\theta)^{\frac{1}{2}}\xi+\tfrac{3}{2}\sin^2\theta\cdot\xi^2 \mp\frac{\frac{3}{2}\sin^2\theta}{(1+3\sin^2\theta)^{\frac{1}{2}}}(1-3\sin^2\theta)\xi^3 +\tfrac{3}{8}(4\sin^2\theta-3\sin^4\theta)\cdot\xi^4 \mp\frac{3}{8}\frac{\sin\theta}{(1+3\sin^2\theta)^{\frac{1}{2}}}(4-45\sin^2\theta -81\sin^4\theta+162\sin^6\theta)\xi^5+\cdots\Big], \tag{8a}$$

$$E_{[\frac{3}{2}]D,\,[\frac{3}{2}]C}=-\Big[-1\mp3\cos\theta\cdot\xi-\tfrac{3}{2}\sin^2\theta\cdot\xi^2 \pm\tfrac{3}{2}\sin^2\theta\cdot\cos\theta\cdot\xi^3-\tfrac{3}{8}(4\sin^2\theta-3\sin^4\theta)\cdot\xi^4 \mp\frac{3}{8}\frac{\sin^2\theta(-4+\sin^2\theta+4\sin^4\theta)}{\cos\theta}+\cdots\Big], \tag{8b}$$

where the levels A and B, C and D are still grouped as $[\frac{1}{2}]$ and $[\frac{3}{2}]$ levels because the magnetic energy is small compared to the quadrupole interaction energy (i.e., $\xi\ll1$). The appearance of $\cos\theta$ in the denominator shows that the last series diverges if $\theta=90°$.

These four levels are plotted in Fig. 1 for $\theta=0°$ to 90° as the set of solutions as a whole is evidently symmetric about 90°. When $\theta\neq0°$, the four Zeeman components $A\to D$, $A\to C$, $B\to D$, $B\to C$ are allowed magnetic-dipole transitions and their frequencies may be calculated from Eqs. (8a) and (8b). According to the original matrix equation (2), there is a particular orientation at which the two Zeeman components f_{BD}, f_{AC} coincide. For any value of η, this orientation is given by

$$2-3\sin^2\theta+\eta^2\sin^2\theta\cos2\phi=0. \tag{9}$$

When $\eta=0$, or when $\phi=\pm45°$, $\pm135°$, coincidence occurs at $\theta=\sin^{-1}(\sqrt{\frac{2}{3}})=54.7°$.

(iv) For an external magnetic field perpendicular to the electric symmetry axis or $\theta=90°$ ($\eta=0$),

$$E_{[\frac{1}{2}]B,\,[\frac{1}{2}]A}=-(1\mp2\xi+4\xi^2)^{\frac{1}{2}}\pm\xi=-\Delta_{\mp}\pm\xi, \tag{8c}$$

$$E_{[\frac{3}{2}]D,\,[\frac{3}{2}]C}=(1\mp2\xi+4\xi^2)^{\frac{1}{2}}\pm\xi=\Delta_{\mp}\pm\xi, \tag{8d}$$

where

$$\Delta_{\mp}=(1\mp2\xi+4\xi^2)^{\frac{1}{2}}. \tag{8e}$$

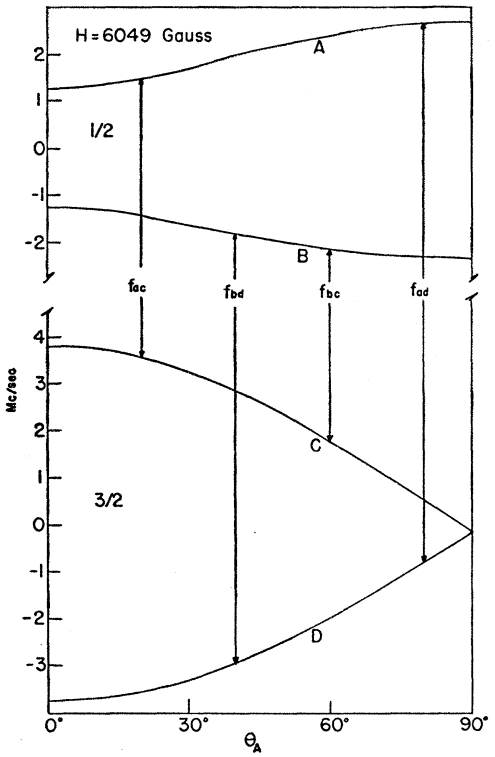

FIG. 1. Energy level diagram showing splitting of the nuclear quadrupole levels in a strong magnetic field for various angles θ_A between H field and the axis of electric symmetry. The separation between the $[\frac{1}{2}]$ and $[\frac{3}{2}]$ levels in the absence of a perturbing H field is 29.903 Mc/sec.

For $\xi \ll 1$, the spacing between levels A, B is approximately $4\xi\delta = 2f_M$, while that between levels C, D, is very small, approximately $3\xi^3\delta$. When $\eta \neq 0$, a term linear in magnetic field strength, that is, $\pm\eta\xi$, appears in the solutions of $E_{[\frac{3}{2}]}$. A comparison of level spacing C to D, as deduced from the frequencies of observed Zeeman components f_{BD}, f_{BC}, f_{AD}, f_{AC} at $\theta = 90°$, with $3\xi^3\delta$ therefore should yield an estimation of the asymmetry factor η.

The sodium chlorate crystal is a cubic crystal with four $NaClO_3$ molecules per unit cell.[11] The chlorine nucleus in each molecule is subject to a nonuniform intramolecular electric field with axial symmetry along the $Na^+ - ClO_3^-$ axis. Thus, for each Cl nucleus in the unit cell there is a different axis of electric symmetry. The arrangement of the $NaClO_3$ molecules in the unit cell is such that the axis of electric symmetry for each Cl nucleus is parallel to a body diagonal of the unit cell (i.e., perpendicular to the 111 plane).

Thus, for a single crystal in a magnetic field there are usually four Zeeman patterns corresponding to the four symmetry axes. Each pattern may contain four Zeeman components f_{AC}, f_{AD}, f_{BC}, and f_{BD} in the vicinity of the zero field line f_0 as indicated in Fig. 1. Thus, for weak magnetic fields, it is usually difficult to distinguish the lines of a given pattern from overlapping lines belonging to other patterns. For a few orientations, clear interpretations can be obtained[5,6] but it is not possible to follow unambiguously the detailed behavior of a given pattern as θ and H are varied. By employing strong magnetic fields, detailed studies of a given pattern were made possible.

[11] R. W. G. Wyckoff, *The Structure of Crystals* (Chemical Catalogue Company, New York, 1931), p. 276.

III. EXPERIMENTAL WORK

The $NaClO_3$ crystal employed in the present study was grown from a saturated aqueous solution. By cooling the solution at a rate of approximately 0.5°C per day, it was possible to obtain transparent cubic crystals measuring one inch on an edge in a period of two weeks. Newly prepared crystals were dried and then coated with a protective film of polystyrene. The crystal was mounted in a holder in such a way that one of the body diagonals could be rotated in a horizontal plane. The magnetic field H was horizontal. Since the diagonal of the crystal is along the axis of electric symmetry for one set of Cl nuclei, rotation of the crystal holder provided a method of obtaining all values of θ from 0° to 180° for this set of Cl nuclei. This angle θ will hereafter be denoted by θ_A. For every value of θ_A, there are also three other values of θ belonging to other sets of Cl nuclei; in strong H fields the Zeeman patterns belonging to these other sets of Cl nuclei are easily distinguishable from the pattern being investigated systematically.

The radio-frequency spectrograph utilized an oscillating detector and is similar in essentials to those employed in earlier studies.[12] The detector could be operated either as a super-regenerative detector with external quench or as a regenerative detector with audio

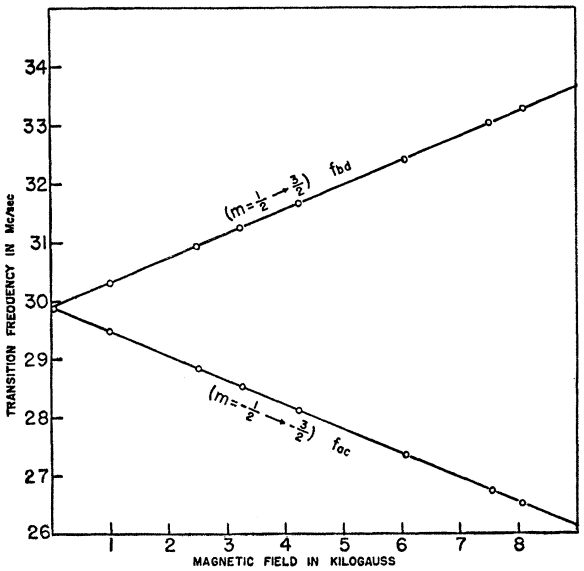

FIG. 2. Observed and calculated splitting of the zero-field quadrupole line as a function of magnetic field for $\theta_A = 0$.

[12] R. E. Sheriff and D. Williams, Phys. Rev. 82, 651 (1951).

feedback.[13] The frequency range covered by the spectrograph was 25 to 35 Mc/sec and a scanning rate as low as 1 kc/sec per minute was employed.

In most of the work, sinusoidal magnetic field modulation at 45 cps was used. However, for certain values of θ_A in the vicinity of 54.7°, frequency modulation of the detector was employed, since for f_{AC} and f_{BD} components Zeeman modulation produces only second-order effects at this value of θ_A; this may be seen from Eqs. (8a) and (8b).

Frequency measurements were made by means of a frequency standard calibrated by signals from WWV. When the super-regenerative detector was employed, the central frequency was determined by means of the frequency standard and an auxiliary receiver, which was used to "track" the central frequency. Under widely different quench conditions, the line frequency measurements were reproducible to within ±1 kc/sec.

Magnetic field measurements were made in terms of the magnetic resonance frequencies of H^1 in water and Li^7 in aqueous LiCl solution. In these measurements the following effective g-values were assumed: $g(H^1)=5.58536$ and $g(Li^7)=2.17063$. The resonance frequency values were reproducible to one part in 20 000.

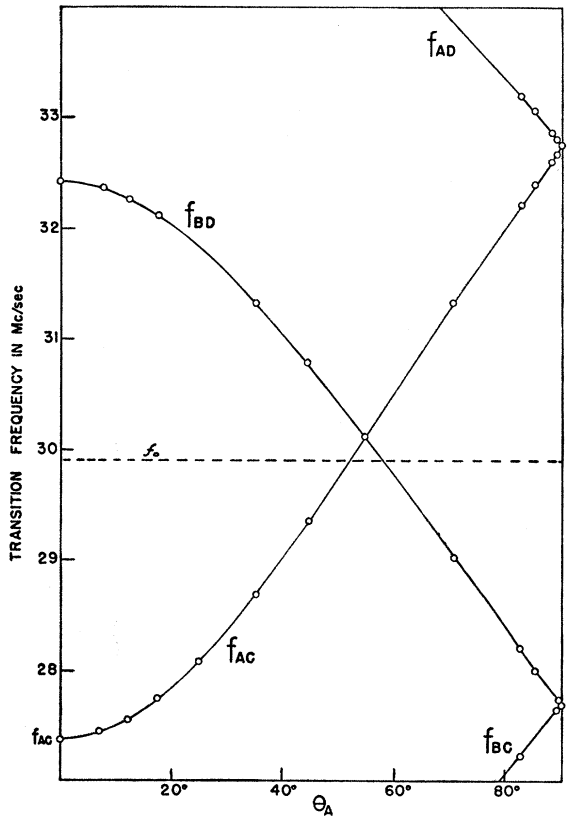

FIG. 3. Observed and calculated frequencies of Zeeman components of a field of 6049 gauss at various orientations θ_A.

[13] T. C. Wang, Doctoral dissertation, Columbia University, 1953 (unpublished).

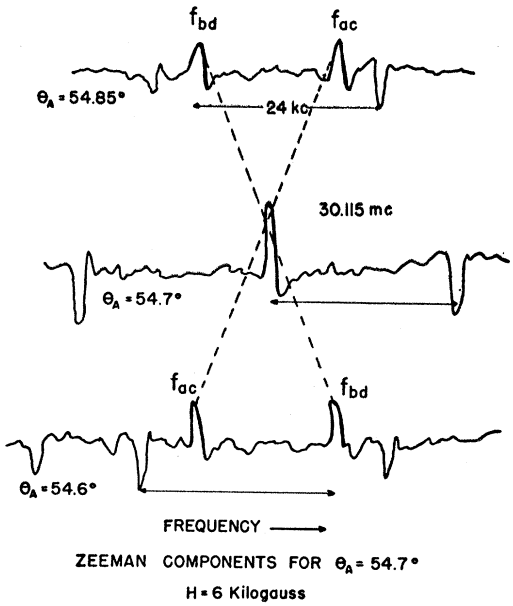

FIG. 4. Observed Zeeman components f_{AC} and f_{BD} in the vicinity of $\theta_A=54.7°$. Super-regenerative sideband peaks spaced at 24-kc/sec intervals are useful for direct measurement of small frequency differences.

Values for angle θ_A could be determined from a divided circle mounted on the shaft of the crystal holder. From the divided circle, θ_A could be measured to ±0.1°. Near angles of special interest such as 54.7° and 90°, angle measurements with an auxiliary tangent-drive micrometer were used to measure $\Delta\theta_A$ to ±0.01°. The exact divided circle reading corresponding to $\theta_A=0°$ was determined by observing the crystal orientation at which f_{AC} had its minimum value and f_{BD} had its maximum for a given strong H field.

All spectra were obtained with the sample at room temperature, which varied from 36°C to 25°C over a period of several months. As the quadrupole transition frequencies in a given sample show a slight variation with sample temperature, it was necessary to reduce all observed frequencies to the values corresponding to a sample at some arbitrary "standard" temperature. A temperature of 30°C was chosen for this purpose and a temperature coefficient of −4 kc/sec per °C was employed. This coefficient, which was actually obtained with the single crystal employed in most of the work, is in excellent agreement with that obtained in earlier studies.[6,13]

IV. RESULTS

The results of the present work for the case of zero external magnetic field give a value of $f_0=29.903$ ±0.001 Mc/sec for a single $NaClO_3$ crystal at 30°C. This value is in agreement with earlier work[6,13] and yields a value of $|\delta|=14.952$ Mc/sec in Eq. (4), or a value of $|e^2Qq|=59.806$ Mc/sec on the assumption that $\eta=0$.

The results obtained for a crystal with orientation

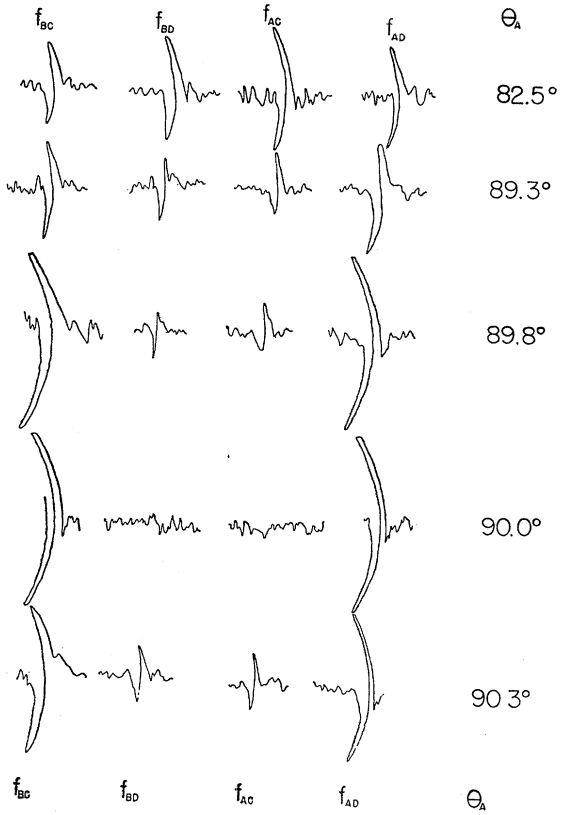

FIG. 5. Intensity variations of Zeeman components f_{AC}, f_{AD}, f_{BC}, and f_{BD} in the vicinity of $\theta_A=90°$ in a field of 6 kilogauss.

$\theta_A=0°$ in a magnetic field are summarized in Fig. 2. The solid curves give the frequencies predicted from Eq. (7a) when the value $\delta=14.952$ Mc/sec is used and when the magnetic moment $\mu_{Cl^{35}}=0.820896\pm0.000050$ n.m. obtained in measurements of LiCl solutions is employed without diamagnetic correction.[14] The circles in Fig. 2 represent the frequencies of the observed Zeeman components. The agreement between observed and predicted values is excellent and indicates that $\eta<0.08$ in Eq. (7b). Precise measurements at two widely different values of the H field suggests that agreement between observed and predicted values can further be improved by using a value $\mu_{Cl^{35}}=0.8215\pm0.0001$ n.m. This value of $\mu_{Cl^{35}}$ is closer to the diamagnetically corrected value $\mu_{Cl^{35}}=0.82180\pm0.00005$ n.m. than to the uncorrected value obtained in LiCl solutions.[14]

The frequencies of the Zeeman components obtained for various angles θ_A in a magnetic field of approximately 6 kilogauss are shown in Fig. 3. The solid curves represent frequencies calculated from Eqs. (8a) to (8d) with the same values for electric quadrupole and magnetic dipole interactions used to obtain the solid curves in Fig. 2. The circles represent observed frequencies. The agreement between observed and calculated frequencies is excellent without introducing an asymmetry factor.

It will be noted from Fig. 3 that f_{AC} and f_{BD} converge in the vicinity of 54.7°. The behavior of the Zeeman components in the vicinity of 54.7° is illustrated in Fig. 4, which shows recorder tracings for three angles near 54.7°. This convergence indicates that $\eta=0$ in Eq. (9) or $\phi=\pm45°$ or $\pm135°$. It seems very likely that η is extremely small or indeed zero, since the actual frequency as calculated for $\theta_A=54.7°$ is 30.116 Mc/sec if $\eta=0$ and the observed value is 30.115 ± 0.001 Mc/sec.

The Zeeman components f_{AD} and f_{BC} were observed between $\theta_A=80°$ and 90°; for $\theta_A=0$, these components are forbidden transitions for magnetic dipole radiation but become very intense as θ_A approaches 90°. The intensities of Zeeman components f_{AC} and f_{BD} decrease as θ_A approaches 90°. The behavior of the various Zeeman components is shown in Fig. 5 in which there are reproduced recorder tracings obtained for various values of θ_A in the vicinity of 90°. The behavior of all lines is symmetric about $\theta_A=90°$ and in Fig. 3, predicted frequencies are given only for the region from 0° to 90°. However, Fig. 5 includes one tracing for $\theta_A=90.3°$ to demonstrate that symmetry does exist. It will be noted that Zeeman components f_{AC} and f_{BD} disappear in the noise at $\theta_A=90°$ and that components f_{AD} and f_{BC} have maximum intensity at $\theta_A=90°$.

The variation in the intensities of the Zeeman components can be understood from a consideration of transition probabilities at $\theta_A=90°$. The transformation matrix which diagonalizes the Hamiltonian matrix of Eq. (2) at $\theta_A=90°$ and for $\eta=0$ can be obtained in closed form. If the arbitrary angle ϕ_A (arbitrary because $\eta=0$), is chosen to be zero (i.e., H along the x axis), the transformation matrix is

$$\|\langle i|m\rangle\|=\frac{\sqrt{3}\xi}{2}\cdot\begin{array}{c}\\ (D)\end{array}\begin{array}{|cc|}\multicolumn{2}{|c|}{(E_{D,B}-\xi)^{-\frac{1}{2}}(E_{D,B}-1)^{-\frac{1}{2}}\begin{bmatrix}1\\ \dfrac{E-1}{\sqrt{3}\xi}\\ \dfrac{E-1}{\sqrt{3}\xi}\\ 1\end{bmatrix}_{D,B}} & \multicolumn{2}{c|}{(E_{A,C}+\xi)^{-\frac{1}{2}}(E_{A,C}-1)^{-\frac{1}{2}}\begin{bmatrix}1\\ \dfrac{E-1}{\sqrt{3}\xi}\\ \dfrac{1-E}{\sqrt{3}\xi}\\ -1\end{bmatrix}_{A,C}}\end{array}\begin{array}{l}(\tfrac{3}{2})\\ (\tfrac{1}{2})\\ (-\tfrac{1}{2})\\ (-\tfrac{3}{2})\end{array}\qquad(10)$$

$$\begin{array}{cccc}(D) & (B) & (A) & (C)\end{array}$$

[14] Yu Ting and D. Williams, Phys. Rev. 89, 595 (1953).

TABLE I. Frequencies (kc/sec) of Zeeman components in the neighborhood of 54.7°. $H=6049$ gauss.

	Observed frequency				Calculated frequency				Deviation (Obs.-Calc.)			
θ_A	f_{BD}	f_{AC}	Diff.	Mean	f_{BD}	f_{AC}	Diff.	Mean	f_{BD}	f_{AC}	Diff.	Mean
54.60°	30 126	30 108	18	30 117	30 125	30 106	19	30 115	1	2	−1	2
54.66°	30 118	30 111	7	30 115	30 120	30 112	8	30 116	−2	−1	−1	−1
54.70°	30 115	30 115	0	30 115	30 116	30 116	0	30 116	−1	−1	0	−1
54.85°	30 107	30 125	−18	30 115	30 108	30 125	−17	30 117	−1	0	−1	−2
55.20°	30 082	30 153	−71	30 118	30 085	30 152	−67	30 119	−3	1	−4	−1

where $|i\rangle=|A\rangle, |B\rangle, |C\rangle, |D\rangle$ are eigenstates belonging to the energy levels given in Eqs. (8c) and (8d). By the choice of $\phi_A=0$, the radio-frequency magnetic field is then along the y axis. Hence the matrix elements which determine the probability of magnetic-dipole transitions between the states $|B\rangle$ and $|C\rangle$, $|B\rangle$ and $|D\rangle$, $|A\rangle$ and $|C\rangle$, $|A\rangle$ and $|D\rangle$ are

$$\begin{aligned}
&\frac{1}{i}\langle C|I_y|B\rangle=\tfrac{1}{4}[(E_C+\xi)(E_B-\xi)(E_C-1)(E_B-1)]^{-\frac{1}{2}}[3\xi(E_C-E_B)+2(E_C-1)(1-E_B)]\\
&\qquad=\frac{\sqrt{3}}{2}(1+\xi+\cdots)=\frac{1}{i}[\langle C|I_y|A\rangle]_{\theta_A=0}(1+\xi+\cdots),\\
&\frac{1}{i}\langle B|I_y|D\rangle=\tfrac{1}{4}[(E_D-\xi)(E_B-\xi)(E_D-1)(E_B-1)]^{-\frac{1}{2}}\left[\frac{3\xi}{2}(E_D-1-E_D+1)+(E_B-E_B-1+1)\left(E_D-1-\frac{3\xi}{2}\right)\right]\\
&\qquad=0,\\
&\frac{1}{i}\langle C|I_y|A\rangle=\tfrac{1}{4}[(E_C+\xi)(E_A+\xi)(E_C-1)(E_A-1)]^{-\frac{1}{2}}\left[\frac{3\xi}{2}(E_C-1-E_C+1)+(E_C-1+1-E_C)\left(E_C-1-\frac{3\xi}{2}\right)\right] \qquad (11)\\
&\qquad=0,\\
&\frac{1}{i}\langle A|I_y|D\rangle=\tfrac{1}{4}[(E_D-\xi)(E_A+\xi)(E_D-1)(E_A-1)]^{-\frac{1}{2}}[3\xi(E_D-E_A)-2(E_D-1)(1-E_A)]\\
&\qquad=\frac{\sqrt{3}}{2}(1-\xi+\cdots)=\frac{1}{i}[\langle B|I_y|D\rangle]_{\theta_A=0}(1-\xi+\cdots).
\end{aligned}$$

This shows that the intensities of the two Zeeman components f_{BD} and f_{AC} at $\theta_A=90°$ should indeed be zero.

Moreover this equation, together with considerations of the frequency values, shows that the other two Zeeman components at $\theta_A=90°$, f_{BC} and f_{AD}, should be equal in intensity (up to the second power of ξ) to the two allowed Zeeman components at $\theta_A=0$, f_{BD}, and f_{AC}, respectively. For a field of 6 kilogauss, $\xi=8$ percent, the f_{BC} component should be 16 percent stronger than the f_{AD} component. The recorded trace at 90° shows that they are of the same order of magnitude.

An attempt to measure the line widths of f_{AC} and f_{BD} at $\theta_A=0$ in fields of 3 and 6 kilogauss was made by means of a regenerative detector. The results obtained indicate that the frequency interval between points of maximum and minimum slope as shown on recorder tracings was 900±100 cps at room temperature. No difference in line width was noted when the field was changed from 3 to 6 kilogauss. This result suggests that a major part of the line width may be due to small variations in crystalline field throughout the sample.

V. DISCUSSION OF RESULTS

From the data presented in Figs. 2 and 3 it can be seen that there is excellent agreement between observed frequencies and frequencies calculated from theory on the assumption of complete axial symmetry with e^2Qq obtained from zero field measurements and μ from resonance experiments on LiCl solutions. In order to investigate possible differences between observed and calculated frequencies and to obtain an upper limit for the asymmetry factor η, details of the observations at two values of θ_A were given special attention.

Table I gives a comparison of observed and predicted frequencies near $\theta_A=54.7°$. The column headed "Diff." in the table of observed values gives precise frequency differences as obtained from the spacing of super-

TABLE II. Splitting of the $[\frac{3}{2}]$ level in 90° neighborhood (kc/sec).

	Observed splitting		Calculated splitting
θ_A	$f_{AD}-f_{AC}$	$f_{BD}-f_{BC}$	E_C-E_D
	($H=6049$ gauss)		
82.50°	982	983	985
89.32°	92	91	92
89.70°	48	47	47
89.80°	37	36	37
90.00°	(≈30)	(≈30)	27 ($=3\xi^3\delta$)
90.30°	48	48	47
90.88°	117	119	118
	($H=3024$ gauss)		
90.00°	(≈5.5)	(≈6.0)	3.5 ($=3\xi^3\delta$)

regenerative sideband resonances as displayed on the recorder tape. The part of Table I labeled "Deviation" shows that the average deviation between observed and calculated frequency was 1.2 kc/sec. This close agreement near $\theta_A=54.7°$ is to be expected from Eqs. (8a) and (8b), since the calculated frequencies f_{AC} and f_{BD} depend quadratically on ξ and hence are not influenced strongly by the choice of μ. An even closer agreement between observed and calculated frequencies is obtained if one compares the observed and calculated splitting of $[\frac{3}{2}]$ level near 90°, since in Eqs. (8d) and (8b) this splitting involves only ξ^3. Table II gives this comparison.

The splitting of the $[\frac{1}{2}]$ level near 90° depends linearly on ξ. Hence, a comparison of observed and calculated splitting provides a means of checking the value of μ obtained at $\theta_A=0$. Table III gives the comparison when the value of μ obtained with LiCl solutions is used in obtaining the calculated values. It will be noted that the observed splitting is consistently higher than the calculated splitting by approximately 5 kc/sec at 6049 gauss and 2.5 kc/sec at 3024 gauss. In order to bring the observed and calculated values into agreement, it is necessary to set $\mu=0.8216$ nm. This value is in essential agreement with the value $\mu=0.8215\pm0.0001$ nm obtained for $\theta_A=0$.

In connection with Eq. (8d), which was derived for $\eta=0$, it was pointed out that the calculated separation between levels C and D is $3\xi^3\delta$ for $\theta_A=90°$. If $\eta\neq0$, there should be a significant difference between observed splitting, given by $(f_{AD}-f_{AC})$ and $(f_{BD}-f_{BC})$, and calculated splitting at 90°. Unfortunately, the components f_{AC} and f_{BD} disappear at $\theta_A=90°$; however, an extrapolation beyond $\theta_A=89.8°$ is possible. This extrapolation gives a value slightly less than 30 kc/sec for the splitting, as shown in Table II for $H=6049$ gauss. This splitting is to be compared with $3\xi^3\delta=27$ kc/sec. This deviation gives an upper limit of 0.0012 for η. The corresponding comparison for $H=3024$ gauss gives an upper limit of 0.0018 for η. In view of the fact that extrapolation was necessary, η may in fact be zero.

It might be noted from Tables II and III that the agreement between four independent frequency measurements as recorded in the columns giving observed splitting for energy levels is within ±1 kc/sec. This more than justifies the initial estimation of accuracy in spectral line measurements.

TABLE III. Splitting of the $[\frac{1}{2}]$ level in 90° neighborhood (kc/sec).

θ_A	Observed splitting $f_{AD}-f_{BD}$	Observed splitting $f_{AC}-f_{BC}$	Calculated splitting E_A-E_B	Deviation
		($H=6049$ gauss)		
82.50°	4994	4995	4990	5
89.32°	5029	5028	5022.5	6
89.70°	5027	5026	5022	5
89.80°	5026	5025	5022	4
90.00°	...	...	5022	...
90.30°	5026	5028	5022	6
90.88°	5026	5028	5022	5
		($H=3024$ gauss)		
90.00°	2523.2	2523.5	2521.0	2.5

VI. SUMMARY

The results obtained in the present study may be summarized as follows: The total Hamiltonian given in Eq. (1) has proved adequate to account for all observed frequencies to approximately ±1 kc/sec in 30 000 kc/sec and for the observed intensity variations of the various Zeeman components. Three parameters δ, ξ, and η were employed; these parameters involve the following constants:

$$|e^2Qq| = 59.806\pm0.002 \text{ Mc/sec},$$
$$\mu(\text{Cl}^{35}) = 0.8215\pm0.0001 \text{ n.m.},$$
$$\eta < 0.0012.$$

In reducing all experimental data to a single temperature, a temperature coefficient of -4 (kc/sec) per °C was employed.

ACKNOWLEDGMENTS

The writers take pleasure in expressing their appreciation to Professor Preston Harris and Mr. Paul Splitstone of the Chemistry Department for advice on crystal growth, to Professor Duncan McConnell of the Mineralogy Department for advice on cutting of crystals, to Professor Jan Korringa and Dr. C. J. Tsao for helpful consultation on theoretical problems, and to Mr. John Hockenberry for assistance in certain parts of the experimental work.